Experimental observation of the M1 scissors mode in ^{254}No

F.L. Bello Garrote, A. Lopez-Martens, A.C. Larsen, I. Deloncle, S. Péru, F. Zeiser, P.T. Greenlees, B.V. Kheswa, K. Auranen, D.L. Bleuel, et al.

Physics Letters B 834 (2022) 137479

Contents lists available at ScienceDirect

Physics Letters B

www.elsevier.com/locate/physletb

Experimental observation of the $M1$ scissors mode in ^{254}No

F.L. Bello Garrote [a,*], A. Lopez-Martens [b,d,*], A.C. Larsen [a,*], I. Deloncle [b,c], S. Péru [c,d], F. Zeiser [a], P.T. Greenlees [e], B.V. Kheswa [a,1], K. Auranen [e], D.L. Bleuel [f], D.M. Cox [e,2], L. Crespo Campo [a], F. Giacoppo [g,h], A. Görgen [a], T. Grahn [e], M. Guttormsen [a], T.W. Hagen [a], L. Harkness-Brennan [i], K. Hauschild [b,d], G. Henning [j], R.-D. Herzberg [i], R. Julin [e], S. Juutinen [e], T.A. Laplace [k], M. Leino [e], J.E. Midtbø [a], V. Modamio [a], J. Pakarinen [e], P. Papadakis [e,3], J. Partanen [e,4], T. Renstrøm [a], K. Rezynkina [l,5], M. Sandzelius [e], J. Sarén [e], C. Scholey [e,6], S. Siem [a], J. Sorri [e,7], S. Stolze [e], J. Uusitalo [e]

[a] Department of Physics, University of Oslo, N-0316 Oslo, Norway
[b] Laboratoire de physique des 2 infinis Irène Joliot-Curie, CNRS/IN2P3, F-91405 Orsay Cedex, France
[c] CEA, DAM, DIF, F-91680 Arpajon, France
[d] Université Paris-Saclay, CEA, LMCE, F-91680 Bruyères-le-Châtel, France
[e] University of Jyvaskyla, Department of Physics, P.O. Box 35, FI-40014 University of Jyvaskyla, Finland
[f] Physical and Life Sciences Directorate, Lawrence Livermore National Laboratory, Livermore, CA 94551, USA
[g] Helmholtz Institute Mainz, 55099 Mainz, Germany
[h] GSI Helmholtzzentrum für Schwerionenforschung, 64291 Darmstadt, Germany
[i] Department of Physics, University of Liverpool, Oliver Lodge Laboratory, Liverpool L69 7ZE, United Kingdom
[j] Universitè de Strasbourg, CNRS, IPHC UMR 7178, F-67000 Strasbourg, France
[k] Department of Nuclear Engineering, University of California, Berkeley, CA 94720, USA
[l] CSNSM, IN2P3-CNRS, and Université Paris Sud, Bat. 104-108, F-91405 Orsay, France

ARTICLE INFO

Article history:
Received 3 September 2021
Received in revised form 29 September 2022
Accepted 29 September 2022
Available online 3 October 2022
Editor: B. Blank

Keywords:
Scissors mode
γ-strength function
Transfermium nuclides

ABSTRACT

We present the first experimental evidence of the scissors mode in the superheavy nucleus ^{254}No produced in the ^{208}Pb(^{48}Ca, $2n\gamma$))^{254}No reaction. The spectrum of γ rays emitted by the excited ^{254}No nuclei shows an enhanced γ-ray yield for transition energies of ≈ 2.5 MeV. By measuring the linear polarization properties of the emitted γ rays, we confirm that the transitions in the enhancement region are predominantly of magnetic-dipole character, characteristic for the scissors mode. To further characterize the enhanced γ-ray yield, simulations of the electromagnetic decay of ^{254}No were performed. The observed enhancement is reproduced by including an $M1$ component in the γ strength function with total strength $B(M1\uparrow) = 11.8(19)\ \mu_N^2$. This is in good agreement with the integrated $M1$ strength from sum-rule estimates and new calculations within the quasi-particle random-phase approximation presented here. Our results provide a stringent test of phenomenological formulae for the scissors mode currently used in stellar nucleosynthesis calculations. We find that those formulae are not satisfactory, and we recommend using sum-rule estimates assuming a rigid-body moment of inertia instead for describing the scissors mode in superheavy nuclei.

1. Introduction

The scissors mode is a collective excitation of deformed many-body systems undergoing rotational oscillations. It was first proposed [1] and discovered [2] in the atomic nucleus, and since

* Corresponding authors.
E-mail addresses: f.l.b.garrote@fys.uio.no (F.L. Bello Garrote), araceli.lopez-martens@ijclab.in2p3.fr (A. Lopez-Martens), a.c.larsen@fys.uio.no (A.C. Larsen).

[1] Present address: Department of Physics, University of Johannesburg, P.O. Box 524, Auckland Park 2006, South Africa.
[2] Present address: Department of Physics, Lund University, 22100 Lund, Sweden.
[3] Present address: STFC Daresbury Laboratory, Daresbury, Warrington, WA4 4AD, United Kingdom.
[4] Deceased.
[5] Present address: INFN Sezione di Padova, I-35131 Padova, Italy.
[6] Present address: MTC Limited, Ansty Park, Coventry CV79JU, United Kingdom.
[7] Present address: Radiation and Nuclear Safety Authority - STUK, Jokiniemenkuja 1, 01370 Vantaa, Finland.

https://doi.org/10.1016/j.physletb.2022.137479

then, has been observed in several other many-body systems [3]. Measuring the strength of the scissors mode provides direct information on the moment of inertia of the system. It is therefore an excellent tool to demonstrate the occurrence of superfluidity [4,5]. In the atomic nucleus, the scissors mode manifests itself as a broad peak of magnetic dipole ($M1$) character in the 2-4 MeV region of the γ-strength function (γ-SF), which is, in essence, the probability of the nucleus to deexcite by emitting photons with a certain energy. The presence of the scissors mode in the γ-SF is relevant for stellar nucleosynthesis processes, like the rapid neutron-capture process (r process), as it increases the neutron-capture probability [6–8]. The increment of the neutron-capture probability depends not only on the strength of the scissors mode, but also on its position. In the particular case that the scissors mode lies just above the neutron separation energy, which is plausible for some of the neutron-rich nuclides in the r-process path, the inclusion of the scissors mode in reaction calculations could enhance the neutron-capture cross section by two orders of magnitude [9].

Experimental data indicate that the strength of the scissors mode is larger in heavier nuclides. Total reduced $M1$ strengths, $B(M1\uparrow) = 7.8\text{-}9.8\ \mu_N^2$ [8] were measured in some of the lighter actinides using the Oslo method [10–12]. These values are considerably larger than the ones obtained, for example, in the well deformed $^{160\text{-}164}$Dy nuclides: $B(M1\uparrow) \approx 5\ \mu_N^2$ [13,14]. Sum-rule estimates assuming a rigid-body moment of inertia [10,15] can describe, within errors, the $B(M1\uparrow)$ values measured in the actinides [10–12]. For ^{254}No, the nucleus investigated in this work, the sum rules predict a scissors mode centered at 2.1 MeV with $B(M1\uparrow) = 12.1(13)\ \mu_N^2$, based on the deformation parameter $\beta_2 = 0.27(3)$ reported in Refs. [16–18].

Because of its larger strength, the scissors mode could play an important role in the heaviest nuclides produced in r-process nucleosynthesis. For those nuclides with a sufficiently high fission barrier, an enhancement in the γ-SF due to the presence of a large scissors mode could boost the neutron capture channel relative to fission with subsequent consequences for the synthesis of the heaviest nuclides. Efforts to include the scissors mode in phenomenological formulae used in nuclear reaction codes started only recently [7,19]. The validity of these formulae in the region of the heaviest nuclides, however, is not clear, as the parameters used in the expressions are obtained by comparing to experimental data, which is scarce in this mass region. The observation of the scissors mode is presently not possible for most of the heaviest nuclides, specially for those in the r-process path. ^{254}No is one of the heaviest nuclides that can be produced in the laboratory with a high enough rate [20] to allow for the observation of the scissors mode.

The present work was performed with the following goals: (1) The first observation of the scissors mode in a transfermium nuclide. The unambiguous identification of the scissors mode requires not only the observation of an enhancement of γ-ray intensity in the 2-4 MeV region of the spectrum, but also the experimental verification of its $M1$ character. The present work provides the first direct measurement of the $M1$ character of this enhancement,[9] giving strength to the previous works on the scissors mode in the actinide region [10–12], in which the $M1$ character of the enhancement was just assumed. (2) An estimation of the scissors strength and centroid in ^{254}No. As discussed above, the $B(M1\uparrow)$ strength of the scissors mode and its centroid are presently extrapolated for the heaviest nuclides in r-process path. Although ^{254}No is relatively far from the r-process path, it is the heaviest nuclide for which experimental data on the scissors mode will be available to test currently used phenomenological formulae [7,19].

2. Experimental details

The experiment was performed for a period of two weeks at the Accelerator Laboratory of the University of Jyväskylä. The ^{208}Pb(^{48}Ca, $2n$)^{254}No reaction was employed at two different beam energies of 220 and 222 MeV, with an average beam intensity of 30 pnA, and a target thickness of $\approx 500\ \mu g/cm^2$. At these energies, competing fusion-evaporation channels amount to less than 1% of the total fusion-evaporation cross section [23]. The ^{254}No ions were separated in flight in the gas-filled recoil separator RITU [24,25], and implanted in a pair of double-sided silicon strip detectors (DSSDs) placed at the focal plane of RITU. Prompt γ rays were detected by the Jurogam II germanium-detector array [26], consisting of 15 Compton-suppressed coaxial detectors [27,28] and 24 clover-type detectors [29]. The prompt γ rays were selected in delayed coincidence with recoils detected in the DSSDs. A position-sensitive Multi-Wire Proportional Counter (MWPC) located before the DSSDs, allowed for discrimination between recoils and decay products. Additionally, by measuring the energy loss in the MWPC and the time-of-flight between the MWPC and the DSSDs, it was possible to further discriminate between fusion-evaporation residues and beam or target-like ions that made it through RITU. The ^{154}Sm(^{48}Ca, $6n$)^{196}Pb reaction was also performed during the experiment, as a benchmark for the polarization analysis (see below).

3. Prompt γ-ray spectrum

Previous in-beam measurements on ^{254}No provided information on γ-ray intensity only in the low-energy region [16,17,30–32]. Here we focus on the region above 1 MeV, where the scissors mode is expected. Fig. 1 (top) shows the prompt, recoil-gated, γ-ray singles spectrum obtained for ^{254}No. Gamma rays detected within the same beam pulse in different crystals of the same clover were added together. A ^{56}Co source was used in the energy calibration, providing calibration points up to 3.5 MeV. The spectrum was unfolded following the method described in Ref. [33]. A parametrization of the $E1$ strength described in Ref. [34] is shown in the figure to guide the eye. An enhancement of γ-ray intensity, a "bump-like" structure above a typical, near-exponential spectrum, is noticeable in the region between 1.7 and 3 MeV with centroid at ≈ 2.5 MeV. The singles spectrum obtained using the ^{154}Sm target is shown in Fig. 1 (bottom) for comparison. It originates from the mix of several reaction products: mainly ^{196}Pb (65% [35]) and other Pb, Tl, and Hg nuclides. The spectrum, unfolded in the same manner as the ^{254}No spectrum is, in contrast, essentially featureless above 1 MeV and follows a near-exponential trend. In this case, the absence of the scissors mode is expected, as the spectrum originates from the mix of spherical or weakly deformed nuclides located near the $Z = 82$ shell closure.

The insets in the top panel of Fig. 1 show discrete transitions present in the ^{254}No singles spectrum. The bump at $\approx$ 2.5 MeV appears to be formed by a large group of discrete transitions, similar to what has been previously observed in other actinides [36,37]. However, above 1 MeV, only one transition located at 2808(2) keV stands above the 1.645σ detection limit [38,39]. Below 1 MeV, all the observed transitions have been previously reported [16,17,30–32,40,41].

[8] For consistency, we report here the total $B(M1\uparrow)$ values obtained from the numerical integral of the γ-SF over the entire energy range. See Eq. (19) in Ref. [14].

[9] The $M1$ character of the enhancement in the 2-4 MeV region of the γ-SF of ^{172}Yb [21] was inferred in Ref. [22] by comparing experimentally based, statistical-model calculations to two-step-cascade spectra.

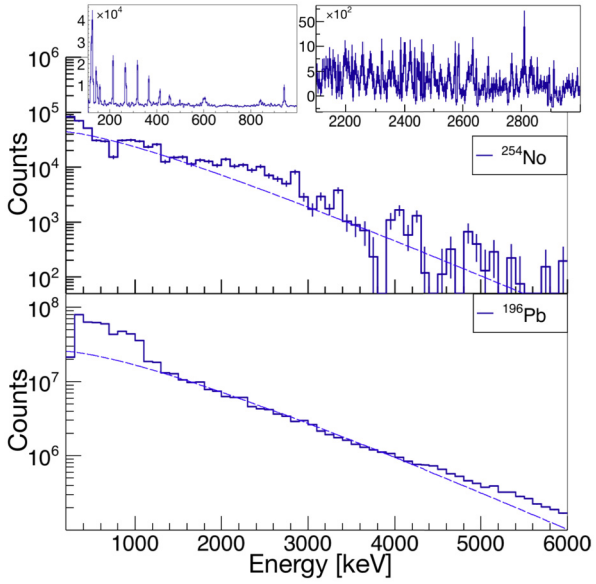

Fig. 1. Prompt, recoil-gated, γ-ray singles spectrum of ^{254}No (top) and ^{196}Pb (bottom), with a bin width of 100 keV. The spectra were unfolded following the method described in Ref. [33]. The insets in the top panel are plotted with a bin width of 4 keV. The dashed lines are fits to the data in the regions of 1.3-1.7 MeV and 3.0-6.0 MeV for ^{254}No, and 1.3-6.0 MeV for ^{196}Pb, using a parametrization of the $E1$ strength described in Ref. [34].

4. Polarization analysis

With the aim of obtaining an experimental confirmation of the magnetic character of the enhancement of γ-ray intensity at $\approx$ 2.5 MeV, a linear polarization analysis was performed. In heavy-ion reactions, the excited states populated in the compound nucleus have a certain degree of alignment. Transitions of electric type which depopulate the aligned excited states will predominantly Compton-scatter perpendicular to the beam direction; magnetic transitions, on the contrary, will predominantly scatter parallel to the beam direction [42]. The clover detectors of the Jurogam II array were used in the present work as a Compton polarimeter [43]. Events with two (and only two) γ rays detected in different crystals of the same clover were considered for the analysis. An N_{90} spectrum of predominantly electric transitions was built by adding the energies of those γ rays detected in crystals of the same ring, *i.e.*, with the same zenith angle with respect to the beam direction. Also, an N_0 spectrum of predominantly magnetic transitions was built by adding the energies of those γ rays detected in adjacent crystals which were located in different rings. The spectra were background subtracted using events which were not in coincidence with the detected ^{254}No recoils. The same procedure was performed for the ^{196}Pb data set as a benchmark for the analysis, given the previous linear polarization measurements performed on this nuclide [44]. The N_{90} and N_0 spectra are shown together in Fig. 2 for both ^{254}No and ^{196}Pb.

In the case of ^{196}Pb (Fig. 2 (bottom)), the N_0 spectrum dominates up to $\approx$ 500 keV, from where the N_{90} becomes dominant. This is in accordance with the previous polarization measurements of Ref. [44]. Above 2 MeV, there is no appreciable difference between the two spectra. In ^{254}No (Fig. 2 (top)), three ground-state band transitions located at $\approx$ 300 keV can be observed to be more intense in the N_{90} spectrum. At $\approx$ 2.5 MeV, a broad peak can be observed in the N_0 spectrum.

The predominant magnetic character of the γ rays in the 1.7-3.0 MeV region can be clearly seen by plotting the polarization asymmetry [43]:

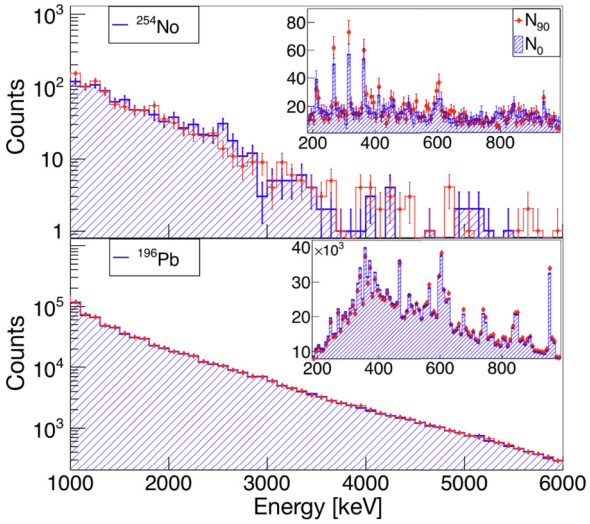

Fig. 2. N_{90} spectrum of transitions scattered perpendicular to the beam direction, and N_0 spectrum of transitions scattered parallel to the beam direction for ^{254}No (top) and ^{196}Pb (bottom), with a bin width of 100 keV. The insets are plotted with a bin width of 4 keV.

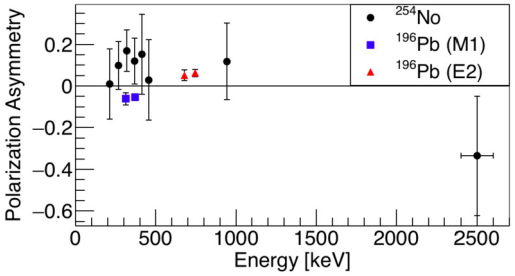

Fig. 3. Polarization asymmetry of the broad peak at $\approx$2.5 MeV, together with the 214-, 267-, 318-, 366-, 412- and 456-keV ground-state band transitions, and the 943-keV transition in ^{254}No. The polarization asymmetry of the $M1$ 314.5- and 374.6- and the $E2$ 679.2- and 745.2-keV transitions in ^{196}Pb is shown for comparison.

$$A = \frac{a(E_\gamma)N_{90}^{peak} - N_0^{peak}}{a(E_\gamma)N_{90}^{peak} + N_0^{peak}}, \quad (1)$$

where N_{90}^{peak} and N_0^{peak} are the peak areas in the corresponding N_{90} and N_0 spectra, and $a(E_\gamma)$ is a scaling factor obtained from analyzing unpolarized source data. In the present case $a(E_\gamma) \approx 1$.

The measured polarization asymmetry for the peak at $\approx$ 2.5 MeV is shown in Fig. 3, together with some other discrete, low-energy transitions observed in the spectra. For the background under the peak, the parametrization of Ref. [34] was used. Electric transitions have a positive asymmetry, whereas magnetic transitions have a negative asymmetry. The points below 500 keV correspond to pure $E2$ transitions in the ground-state band, and they display a positive asymmetry. For the peak at $\approx$ 2.5 MeV, a relatively large negative asymmetry can be observed.

5. Simulations

The bulk features observed in the experimental spectrum of Fig. 1 are determined by the level density and the γ-SF of the nucleus, together with the entry distribution, *i.e.*, the distribution of initial spin and excitation energy of the nucleus, before γ decaying to the ground state. To investigate the influence of these quantities in the observed structure at $\approx$ 2.5 MeV, the prompt γ-ray spectrum was simulated using different models for the level density

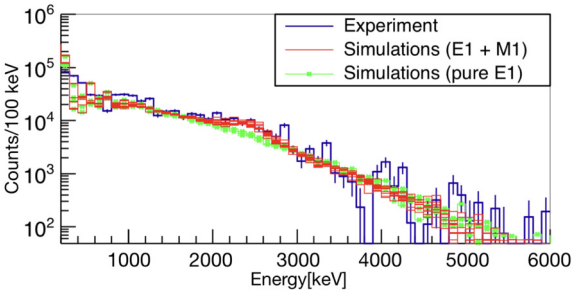

Fig. 4. Experimental spectrum of ^{254}No compared to simulated spectra with and without the $M1$ scissors mode. See the text for more details.

and the γ-SF, together with the entry distribution experimentally obtained in Ref. [45].

The simulations were performed with the code RAINIER [46], a Monte Carlo based simulation tool for modeling γ-ray cascades. The code builds as a first step a set of randomly generated nuclear levels based on a given level density model. The known level scheme up to a user-defined energy can be specified, and it is assumed by the code to be complete. This set of nuclear levels is called a "realization". After the realization is built, levels are populated based on a given entry distribution, and the γ-ray cascades to the ground state are simulated using γ-SF models for $E1$, $M1$, and $E2$ transitions. Two different models for the level density were used in the simulations: the Constant Temperature (CT) [47] and the Back Shifted Fermi Gas (BSFG) models [48,49], with parameters $T = 0.432$ MeV, $E_0 = -0.240$ MeV for the former, and $a = 25.208$ MeV^{-1}, $E_1 = 0.288$ MeV for the latter [50]. Energy levels in the ground-state band up to the 10^+ state [16,17,30–32] were specified. At higher energies, the level scheme cannot be assumed to be complete anymore and the levels were randomly generated according to the level density model. The chosen entry distribution was the average of the two distributions measured in Ref. [45] for beam energies of 219 and 223 MeV.[10] The $E1$ γ-strength was modeled either with a Standard Lorentzian (SLO) or an Enhanced Generalized Lorentzian (EGLO), using the following parameters for the double-humped giant dipole resonance: $\sigma_1 = 526$ mb, $E_1 = 10.77$ MeV, $\Gamma_1 = 2.39$ MeV, and $\sigma_2 = 263$ mb, $E_2 = 13.72$ MeV, $\Gamma_2 = 3.77$ MeV [51]. A standard Lorentzian of $M1$ character centered around 2.5 MeV was added to the γ-strength function. Over 2100 spectra were simulated with the BSFG + $E1$ SLO + $M1$ model combination, using selected values of the cross section (σ), centroid (ω) and width (Γ) of the $M1$ Lorentzian. Similarly, 1000 spectra were simulated with the CT + $E1$ EGLO + $M1$ combination. Ten different realizations were simulated for each parameter selection, and each realization was populated 7000 times, resulting in spectra with 3.8-5.8 $\times 10^4$ γ-ray events. The total number of events in the raw experimental spectrum was $\approx 4.6 \times 10^4$. The total $B(M1\uparrow)$ strength added to the simulated spectra was in the range of $\approx$ 4.5-31 μ_N^2. The simulated spectra were compared to the data by evaluating a χ^2 function (see Ref. [52] for details).

Ten simulated spectra corresponding to the 10 lowest χ^2 values (χ^2 ranging from 134 to 143) are shown in Fig. 4. They correspond to the BSFG + $E1$ SLO + $M1$ SLO model combination. The $B(M1\uparrow)$ strengths of these 10 best simulations are in the range of 8.6-16.7 μ_N^2. The parameters of the $M1$ Lorentzian are in the ranges: $\sigma = 1.2$-2.6 mb, $\omega = 2.4$-2.6 MeV and $\Gamma = 0.3$-0.6 MeV. Simulations corresponding to the BSFG + $E1$ SLO model combination, in this case with no $M1$ strength, are also shown for comparison.

[10] The current data was obtained employing the same reaction and target thickness, with beam energies of 220 and 222 MeV.

Large deviations can be observed in the low-energy part of the simulated spectra, below ≈ 1 MeV. It is difficult to describe this region accurately using statistical models, and the available information on the low-lying level structure of the nucleus is not enough to provide a sufficiently complete level scheme to the code. Therefore, the simulated spectra were scaled to the experimental spectrum in the region between 1.3 and 1.7 MeV, where there is no apparent excess of intensity, and the spectrum should be dominated by the $E1$ statistical "background".

The analysis [52] of the simulated spectra indicates that the data is best reproduced by adding an $M1$ Lorentzian with total $B(M1\uparrow) = 11.8(19)$ μ_N^2. This value agrees very well with the sum-rule estimate $B(M1\uparrow) = 12.1(13)$ μ_N^2. It is important to remark that the former $B(M1\uparrow)$ value was obtained from those simulations based on the SLO model for the $E1$ strength. It is therefore model dependent and should only be considered as an estimation. The simulations performed with the EGLO model do not seem to converge in an optimal $B(M1\uparrow)$ strength [52], as it was the case for the SLO model. The most likely reason is the absence of spin-flip and pygmy resonances in the simulations. The γ-SF in the case of the lighter actinides [10–12] was fit using the EGLO model, but spin-flip and pygmy resonances were introduced to fit the experimental points. The summed strength of these resonances accounted for about 1/3 of the total strength at $\approx$4 MeV. In our case, without experimental values of the γ-SF, it is not prudent to add spin-flip and pygmy resonances to the model. However, the SLO model provides a relatively larger $E1$ strength in the 1-4 MeV region that can compensate for the absence of spin-flip and pygmy resonances [52]. The very good agreement with the sum-rule estimate (in line with the results of the lighter actinides [10–12]), together with the results of the QRPA calculations (see below), gives us confidence in our estimated $B(M1\uparrow)$ value.

6. Comparison with theory and phenomenological formulae

The estimated $B(M1\uparrow)$ strength is shown in Fig. 5 together with Gogny axially-symmetric-deformed Hartree-Fock-Bogolyubov (HFB) plus quasi-particle random-phase approximation (QRPA) [53] results. The present calculations were performed with the D1M effective interaction using $N_0 = 15$ major shells and an energy cut-off of 90 MeV that ensures the convergence. After applying a shift toward lower energies following Ref. [54], the centroid is found at 2.4 MeV in good agreement with the experiment. The summed QRPA $B(M1\uparrow)$ strength is 9.0 μ_N^2. The integrated $B(M1\uparrow)$ strength of the estimated Lorentzian in the region where the calculated states are found (1.8-2.9 MeV) is 9.2 μ_N^2, which compares very well with the QRPA summed strength. QRPA calculated states, however, are normally folded by Lorentzian functions and the total strength is renormalized for their use in nuclear reaction codes [6,8]. In Ref. [8], after this procedure, the γ-SF in the region of the scissors mode is underestimated by a factor of ≈ 2 in the actinides.

Fig. 5 also shows the $B(M1\uparrow)$ strengths obtained using the phenomenological formulae described in Refs. [7,19]. The total $B(M1\uparrow)$ strength obtained from Ref. [7] is 28.2 μ_N^2, largely exceeding our estimated value, and the centroid is found at 3.4 MeV. The reason for the large $B(M1\uparrow)$ strengths obtained in Ref. [7] is the use of the GLO model that gives a much lower $E1$ strength in the region of the scissors mode. In the case of the formula from Ref. [19], the total $B(M1\uparrow)$ strength is 6.3 μ_N^2, and the centroid is found at 2.9 MeV. This formula is obtained by performing a fit to QRPA values from Ref. [8], therefore, the underestimation by a factor of ≈ 2 of the $B(M1\uparrow)$ strength in ^{254}No can be expected.

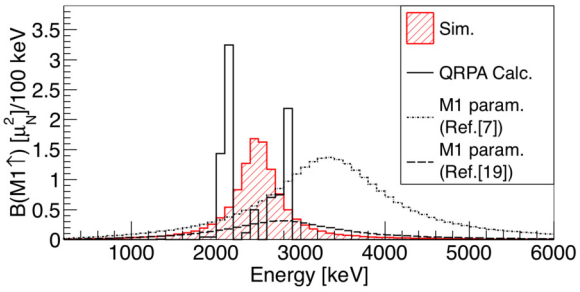

Fig. 5. $B(M1\uparrow)$ strength estimated from the simulations together with the results of the QRPA calculations and the parametrizations in Refs. [7,19].

7. Conclusions

In this work, we have evidenced an enhancement of the γ-ray yield in the 1.7-3.0 MeV region of the ^{254}No spectrum. A linear polarization analysis has demonstrated the predominant magnetic character of the excess yield, suggesting that the observed enhancement of γ-ray intensity is due to the $M1$ scissors mode. The total estimated strength of the scissors mode, $B(M1\uparrow) = 11.8(19)\ \mu_N^2$, is in good agreement with the sum-rule estimates. QRPA calculations were presented in this work, and were in agreement with the estimated strength in the 1.8-2.9 MeV region, where the calculated states are found. These results give support to the previous works in the lighter actinides [10–12], where the strength of the scissors mode in the quasi-continuum region was measured, but its magnetic character was just assumed. The results of two phenomenological scissors-mode formulae that are currently used in nuclear-reaction codes do not compare well with our estimate for the total $M1$ strength. Sum-rule estimates for the scissors mode using the approach of Ref. [19] seem to provide a better description of the γ-SF for the heaviest nuclides. However, using the sum-rule estimates would also require applying a different model for the $E1$ strength in the case of Ref. [7]. More data on other nuclides in the region, like ^{250}Fm, would be highly desirable to confirm that the sum-rule estimates assuming a rigid-body moment of inertia are indeed appropriate for the heaviest nuclides, and to encourage its use in astrophysical calculations.

8. Acknowledgments

The authors would like to thank the staff of the Accelerator Laboratory of the University of Jyväskylä for providing the ^{48}Ca beam during the two weeks of experiment. F. L. B. G., A. C. L., B. V. K., J. E. M. and T. R. gratefully acknowledge funding of this research by the European Research Council through ERC-STG-2014 under grant agreement no. 637686. The use of the GAMMAPOOL loan pool germanium detectors is acknowledged. This work has been supported by the Academy of Finland under the Finnish Centre of Excellence Programme (2012-2017). Support has also been provided by the EU 7th Framework Programme Project No. 262010 (ENSAR), the Norwegian Research Council project 263030 and the UK STFC. This work was performed under the auspices of the U.S. Department of Energy by Lawrence Livermore National Laboratory under Contract DE-AC52-07NA27344.

Declaration of competing interest

The authors declare that they have no known competing financial interests or personal relationships that could have appeared to influence the work reported in this paper.

Data availability

Data will be made available on request.

Appendix A. Supplementary material

Supplementary material related to this article can be found online at https://doi.org/10.1016/j.physletb.2022.137479.

References

[1] N. Lo Iudice, F. Palumbo, Phys. Rev. Lett. 41 (1978) 1532.
[2] D. Bohle, et al., Phys. Lett. B 137 (1984) 27.
[3] K. Heyde, P. von Neumann-Cosel, A. Richter, Rev. Mod. Phys. 82 (2010) 2365.
[4] O.M. Maragò, et al., Phys. Rev. Lett. 84 (2000) 2056.
[5] Tanzi, et al., Science 371 (2021) 1162.
[6] S. Goriely, et al., Phys. Rev. C 94 (2016) 044306.
[7] M.R. Mumpower, et al., Phys. Rev. C 96 (2017) 024612.
[8] S. Goriely, et al., Phys. Rev. C 98 (2018) 014327.
[9] H.P. Loens, et al., Eur. Phys. J. A 48 (2012) 34.
[10] M. Guttormsen, et al., Phys. Rev. C 89 (2014) 014302.
[11] T.G. Tornyi, et al., Phys. Rev. C 89 (2014) 044323.
[12] T.A. Laplace, et al., Phys. Rev. C 93 (2016) 014323.
[13] H.T. Nyhus, et al., Phys. Rev. C 81 (2010) 024325.
[14] T. Renstrøm, et al., Phys. Rev. C 98 (2018) 054310.
[15] J. Enders, et al., Phys. Rev. C 71 (2005) 014306.
[16] P. Reiter, et al., Phys. Rev. Lett. 82 (1999) 509.
[17] M. Leino, et al., Eur. Phys. J. A 6 (1999) 63.
[18] S. Raeder, et al., Phys. Rev. Lett. 120 (2018) 232503.
[19] S. Goriely, V. Plujko, Phys. Rev. C 99 (2019) 014303.
[20] R.-D. Herzberg, et al., Nature 442 (2006) 896.
[21] A. Voinov, et al., Phys. Rev. C 63 (2001) 044313.
[22] A. Schiller, et al., Phys. Lett. B 633 (2006) 225.
[23] S. Eeckhaudt, Spectroscopy in the transfermium region: Probing rotational, non-yrast, and isomeric structures in ^{253,254}No, PhD thesis, University of Jyväskylä, 2006.
[24] M. Leino, et al., Nucl. Instr. Meth. B 99 (1995) 653.
[25] J. Sarén, et al., Nucl. Instrum. Methods A 654 (2011) 508.
[26] P.T. Greenlees, et al., AIP Conf. Proc. 764 (2005) 237.
[27] C.W. Beausang, et al., Nucl. Instrum. Methods A 313 (1992) 37.
[28] C.R. Alvarez, Nucl. Phys. News 3 (1993) 10.
[29] G. Duchêne, et al., Nucl. Instrum. Methods A 432 (1999) 90.
[30] P. Reiter, et al., Phys. Rev. Lett. 84 (2000) 3542.
[31] S. Eeckhaudt, et al., Eur. Phys. J. A 25 (2005) 605.
[32] S. Eeckhaudt, et al., Eur. Phys. J. A 26 (2005) 227.
[33] M. Guttormsen, et al., Nucl. Instrum. Methods A 374 (1996) 371.
[34] S. Leoni, et al., Phys. Lett. B 409 (1997) 71.
[35] O.B. Tarasov, D. Bazin, Nucl. Instr. Meth. B 266 (2008) 4657; A. Gavron, Phys. Rev. C 21 (1980) 230; http://lise.nscl.msu.edu/pace4.
[36] A.S. Adekola, et al., Phys. Rev. C 83 (2011) 034615.
[37] S.L. Hammond, et al., Phys. Rev. C 85 (2012) 044302.
[38] L.A. Currie, Anal. Chem. 40 (1968) 586.
[39] L.E. De Geer, Appl. Radiat. Isot. 61 (2004) 151.
[40] C. Gray-Jones, Isomer spectroscopy of ^{254}No, PhD thesis, University of Liverpool, 2008.
[41] A.J. Ward, In-beam spectroscopy of high-K states in ^{254}No, PhD thesis, University of Liverpool, 2016.
[42] L.W. Fagg, S.S. Hanna, Rev. Mod. Phys. 31 (1959) 711.
[43] P.M. Jones, et al., Nucl. Instrum. Methods A 362 (1995) 556.
[44] A.K. Singh, et al., Nucl. Phys. A 707 (2002) 3.
[45] G. Henning, et al., Phys. Rev. Lett. 113 (2014) 262505.
[46] L.E. Kirsch, L.A. Bernstein, Nucl. Instrum. Methods A 892 (2018) 30.
[47] T. Ericson, Nucl. Phys. 11 (1959) 481.
[48] E. Gadioli, L. Zetta, Phys. Rev. 167 (1968) 1016.
[49] J.R. Huizenga, et al., Phys. Rev. 182 (1969) 1149.
[50] T. von Egidy, D. Bucurescu, Erratum, Phys. Rev. C 72 (2005) 044311, Phys. Rev. C 73 (2006) 049901.
[51] R. Capote, et al., available online at, Nucl. Data Sheets 110 (2009) 3107, https://www-nds.iaea.org/RIPL-3/.
[52] See Supplemental Material at [URL will be inserted by publisher] for details about the simulations with RAINIER.
[53] S. Péru, M. Martini, Eur. Phys. J. A 50 (2014) 88.
[54] M. Kritscka, et al., Phys. Rev. C 99 (2019) 044308.